Supplementary Information (SI) for Physical Chemistry Chemical Physics.
This journal is © the Owner Societies 2026

Supplementary Material

Bandgap Engineering and Edge-State Delocalization in Si-Substituted Zigzag Graphene Nanoribbons for Multilayer p–n Junction Solar Cells: A theoretical Investigation

Ramesh Mamindla[1,2] Srijita Chakraborty[1], and Manish K. Niranjan[1*]

[1]*Department of Physics; Indian Institute of Technology, Hyderabad, TS, 502285, India*

[2]*Department of Physics, VNR Vignana Jyothi Institute of Engineering and Technology, TS, Hyderabad 500118, India*

manish@phy.iith.ac.in

S1. Phonon dispersion and electronic properties

The phonon dispersion of Si doped ZGNR results are calculated using force field potentials and results are illustrated in Fig. S1. The pristine ZGNR phonon is illustrated in Fig. 2. Optical (acousstic) phonons are in the energy range of 150 – 340 meV (0-150 meV). This phonon results of force field potentials are in good agreement with conventional phonon theoretical results which are generally computed using density functional theory (DFT) and density functional perturbation theory (DFPT).[i] The high energy phonons are obtained due to Hydrogen atoms. The phonon dispersion of Si atoms doped ZGNR, as shown in Fig. 1(b). The phonon energies are shifted towards low energy side due to Si atoms as compared to previous case. The Si-C bonds in the Si doped ZGNR are weaker than C-C bonding as a results phonon energy is shifted to lower energy side.

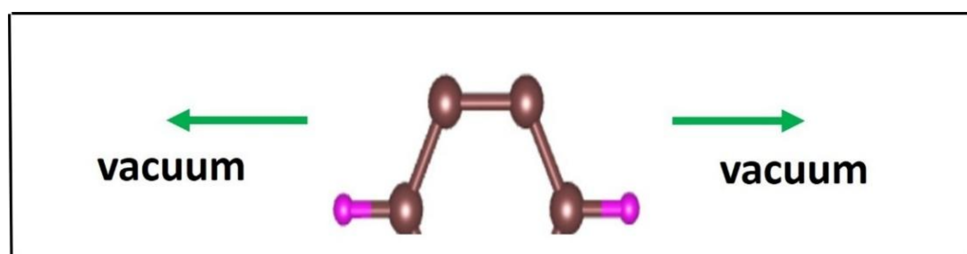

a)

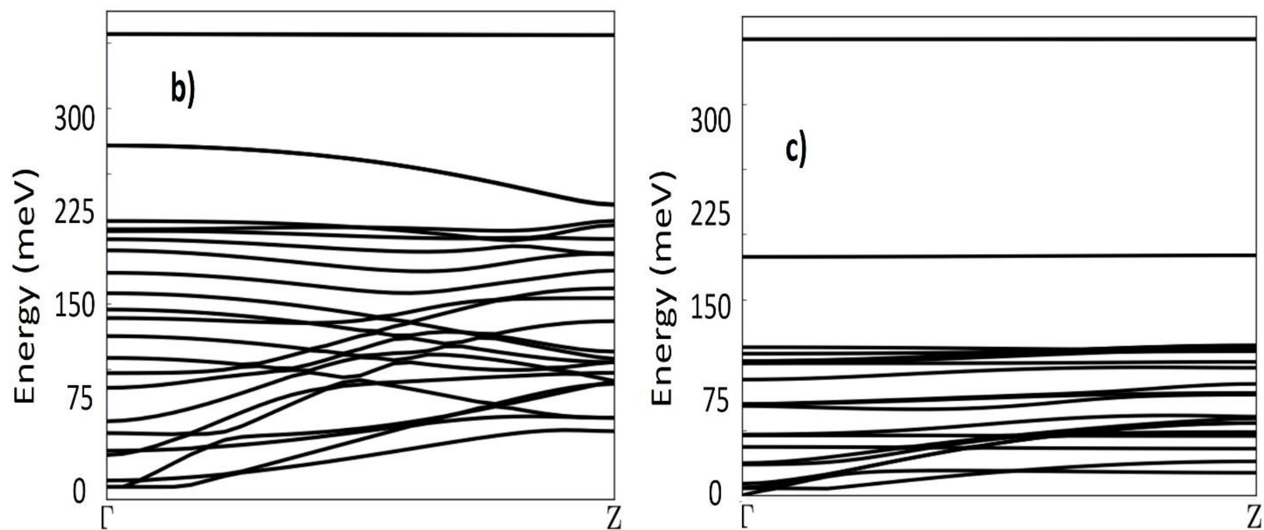

Figure. S1. a) primitive cell of pristine ZGNR. (b) Its phonon dispersion. (c) 2Si substituted ZGNR computed using analytical potentials[ii] .

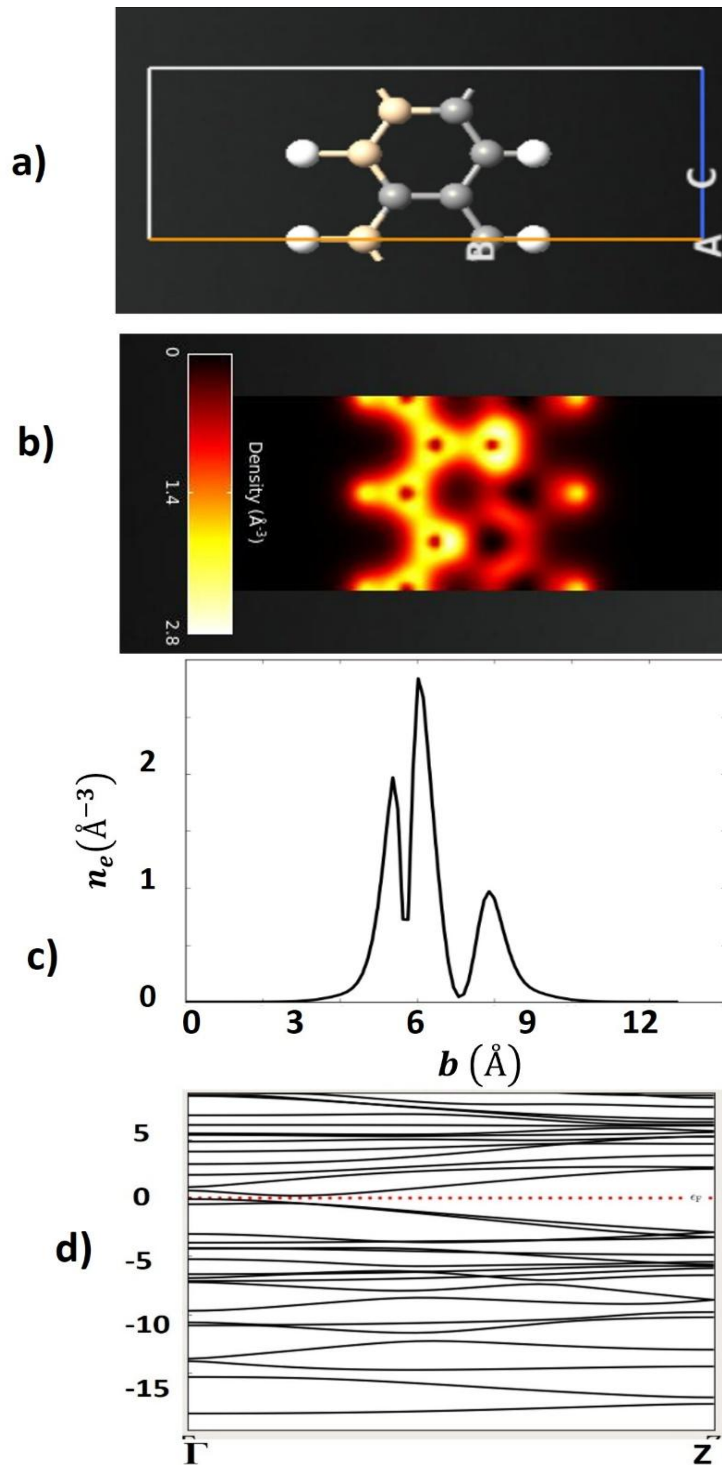

Figure. S2. This is similar to Fig.1 in the case of 3Si doped ZGNR structure, corresponding its charge density in b) & c) band structure. This material has bandgap of 0.25 eV.

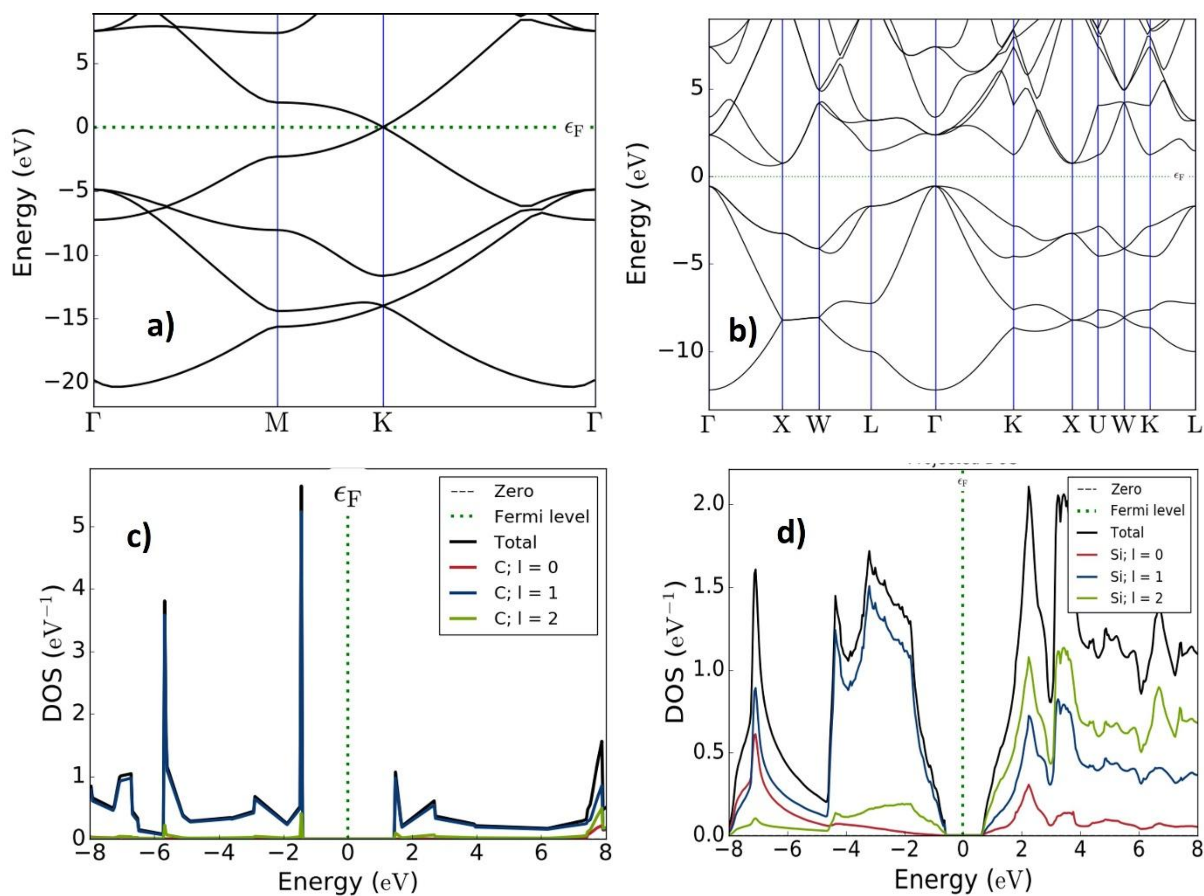

Fig. S3. The computed electronic band structure for **(a)** Graphene **(b)** Silicon. Similarly, density of states for **(c)** Graphene **(d)** Silicon.

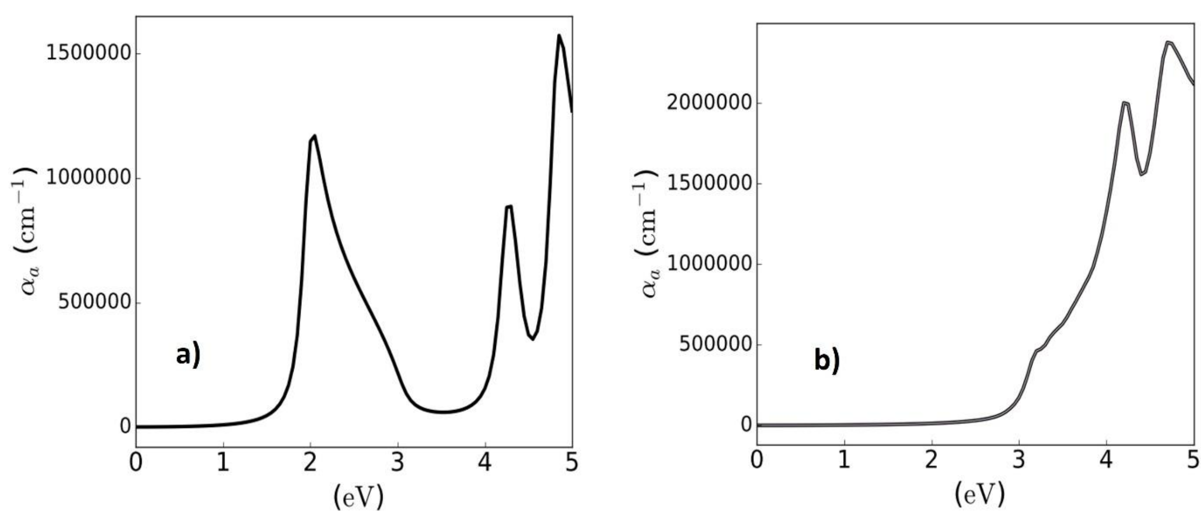

Fig. S4. Computed absorption coefficient for **(a)** Graphene, **(b)** Silicon

S2. Photocurrent of Armchair Graphene nanoribbon

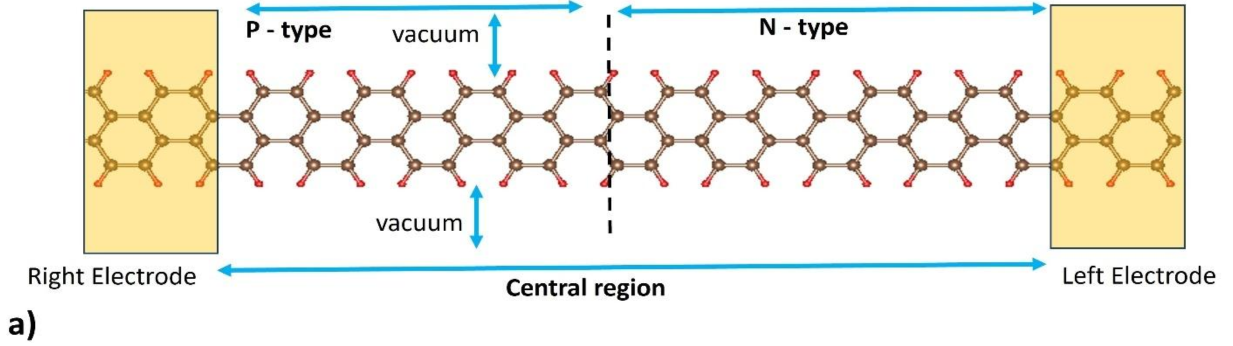

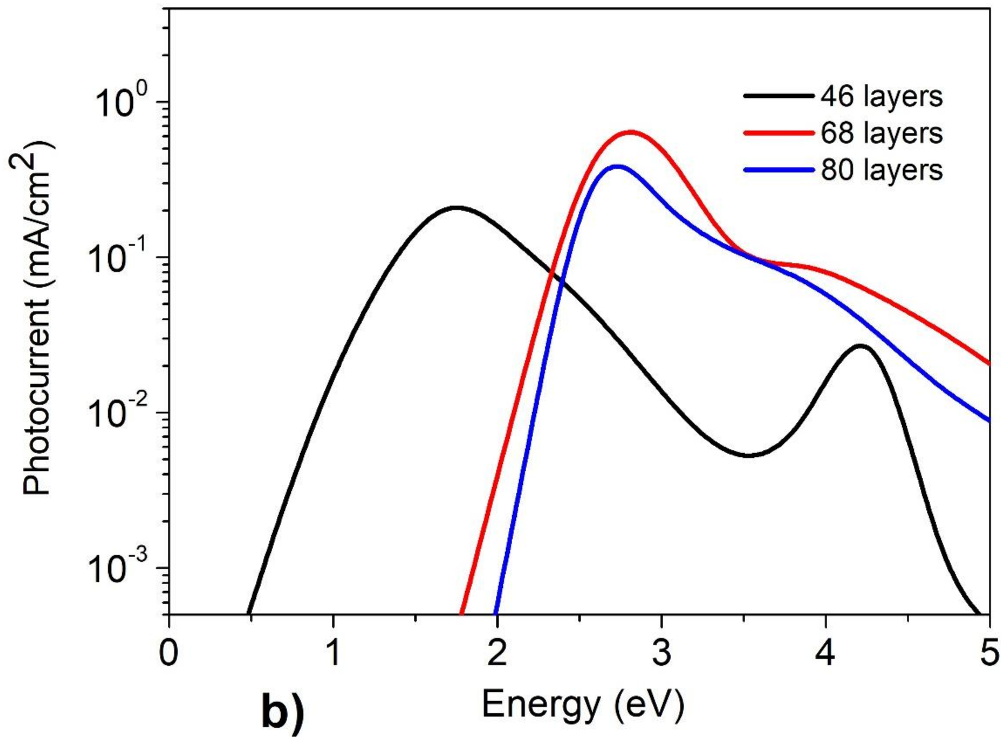

Fig. S5. a) Armchair Graphene nanoribbon p-n junction solar cell device. b) The computed photocurrent of Armchair Graphene nanoribbon p-n junction solar cell device with different atomic layers.

S3. *p-n* junction device structure

The p-n junction device is a two probe supercell structure as shown in Fig. 4 (a). It consists a central region, and right and left electrodes.[14] The central region is sandwiched between electrodes and its length is much larger than that of electrodes. The central region consists very large number of layers whereas each electrode consists less number of layer. The electron charge density in the right and left electrodes are kept same. In case of an applied bias voltage (V_{bias}) across the electrodes, the chemical potentials of right (μ_R) and left (μ_R) electrodes are related as $\mu_{R-}\mu_L = eV_{bias}$. The electron transport direction points from right electrode to the left electrode. An additional charge is added to each atom to model the doping in the device

structure. The first half and second half parts are doped as p-type and n-type, respectively. The p-n junction device structure is used to compute photovoltaic properties in section 3.

S4. Non-equilibrium Green Function (NEGF) method

The NEGF method is used to compute the non-equilibrium electron density[13, 14, 25] in the p-n junction device structure that consists of a central region between left and right electrodes, as shown in Fig. 1(a). There is no coupling between the right and left electrodes because of the large central region. The charge density across the left (L) and right (R) electrodes are written in terms of density matrix (D) as:

$$D = D^L + D^R \quad \text{(S2)}$$

The left/right (L/R) part density matrix can be computed with the NEGF approach as:

$$D^{L/R} = \int \rho^{L/R}(\varepsilon)\, f\left(\frac{\varepsilon-\mu_{L/R}}{k_B T_{L/R}}\right) d\varepsilon \quad \text{(S3)}$$

Where f is the Fermi-Dirac distribution function across the electrodes in terms of the chemical potential of left (right) μ_L (μ_R) electrodes at the temperature T_L (T_R). $\rho^{L/R}$ is spectral density matrix as a function of energy and can be expressed in terms of retarded Green's function (G) and broadening function ($\Gamma^{L/R}$):

$$\rho^{L/R}(\varepsilon) \equiv \frac{1}{2\pi} G(\varepsilon)\Gamma^{L/R}(\varepsilon)G^{\dagger}(\varepsilon) \quad \text{(S4)}$$

The broadening function ($\Gamma^{L/R}$) is related to the self-energies ($\Sigma^{\mathrm{L/R}}$) of the left/right electrodes as:

$$\Gamma^{\mathrm{L/R}} = -\mathrm{i}\left(\Sigma^{\mathrm{L/R}} - \left(\Sigma^{\mathrm{L/R}}\right)^{\dagger}\right) \quad \text{(S5)}$$

The Green's function for the central device region in terms of overlap (S) and Hamiltonian (H) matrices and self-energies ($\Sigma^{\mathrm{L/R}}$) is given as:

$$G(\varepsilon) = [(\epsilon + i\eta)\mathrm{S} - \mathrm{H} - \Sigma^{\mathrm{L}}(\epsilon) - \Sigma^{\mathrm{R}}(\epsilon)]^{-1} \quad \text{(S6)}$$

The transmission coefficient may also be computed from the retarded Green function as:

$$T(\varepsilon) \equiv Tr[G(\varepsilon)\Gamma^L(\varepsilon)G^{\dagger}(\varepsilon)\Gamma^R(\varepsilon)] \quad \text{(S7)}$$

The electric current (I) can be obtained from the transmission function as:

$$I = \frac{2e}{h}\int_{-\infty}^{\infty} T(\epsilon)\left[f\left(\frac{\varepsilon-\mu_L}{k_B T_L}\right) - f\left(\frac{\varepsilon-\mu_R}{k_B T_R}\right)\right] d\epsilon \quad \text{(S8)}$$

The photocurrent, V-I characteristics and other transport properties at finite applied bias voltage can be calculated using the transmission spectrum. More details of the above mentioned NEGF method may be found in Ref. [25]

S5. Photocurrent

In the following we summarize the calculation of Photocurrent with electron-phonon interaction and as implemented in Quantum ATK package [39].

Fig. S6: *p-n* junction device with left and right electrodes

The photocurrent can be computed as a first-order perturbation to the electronic system resulting due to interaction with a weak electromagnetic field [36]. The electron-photon interaction is given by the Hamiltonian.

$$H' = \frac{e}{m_0}\vec{A}\cdot\vec{P} \tag{S10}$$

where $\vec{A}$ and $\vec{P}$ are the vector potential and the momentum operator respectively. For a single-mode monochromatic light source, $\vec{A}$ is given as:

$$\vec{A} = \hat{e}\sqrt{\left(\frac{\hbar\sqrt{\tilde{\mu}_r\tilde{\epsilon}_r}}{2N\omega\tilde{\epsilon}c}F\right)}\left(be^{-iwt} + b^{\dagger}e^{iwt}\right) \tag{S11}$$

Where ω is the frequency of the light, F is the photon flux, N is the number of photons, $\tilde{\mu}_r$ is the relative permeability, $\tilde{\epsilon}_r$ is the relative permittivity, $\tilde{\epsilon}$ is the permittivity, b and $b^{\dagger}$ are the bosonic annihilation and creation operators, and $\hat{e}$ is a unit vector indicating the polarization of the light. Using only first-order terms in F, the current into the left (L) and right (R) leads due to absorption of photons can be expressed as [36]:

$$I_\alpha = \frac{e}{h}\int_{-\infty}^{+\infty}\sum_{\beta=L,R}[1-f_\alpha(E)]f_\beta(E-\hbar\omega)T^{-}_{\alpha,\beta}(E) - f_\alpha(E)\left[1-f_\beta(E+\hbar\omega)\right]T^{+}_{\alpha,\beta}(E)dE, \tag{S12}$$

$$T^{-}_{\alpha,\beta}(E) = N\ \mathrm{Tr}\left\{M^{\dagger}\tilde{A}_\alpha(E)MA_\beta(E-\hbar\omega)\right\}, \tag{S13}$$

$$T^{+}_{\alpha,\beta}(E) = N\ \mathrm{Tr}\left\{M\tilde{A}_\alpha(E)M^{\dagger}A_\beta(E+\hbar\omega)\right\} \tag{S14}$$

Where α indicates the left and/or right lead ($\alpha \in L, R$) shown in Fig. S-I, f_α is the Fermi-Dirac distribution function of lead α, $A_\alpha = G\Gamma_\alpha G^{\dagger}$ is the spectral function of lead α, $\widetilde{A_\alpha} = G^{\dagger}\Gamma_\alpha G$ is the time-reversed spectral function of lead α. The M is the electron-photon coupling matrix and given as

$$M_{ml} = \frac{e}{m_0}\sqrt{\left(\frac{\hbar\sqrt{\tilde{\mu}_r\tilde{\epsilon}_r}}{2N\omega\tilde{\epsilon}c}F\right)}\ \hat{e}\cdot\vec{P}_{ml} \tag{S15}$$

The spectral broadening of the leads α, the retarded G and advanced $G^{\dagger}$ Green's functions, and the momentum operator $\vec{P}$ in semiconductor *p-n* junction device can be calculated self-consistently using DFT and NEGF theoretical framework. The total photocurrent can be computed as $I_{ph} = I_L - I_R$.

The special-thermal-displacement (STD) can be used to include the temperature dependent electron-phonon coupling (EPC) through a single displacement of the atomic positions as:

$$\vec{u}_{\mathrm{STD}}(T) = \sum_\lambda(-1)^{\lambda-1}\vec{e}_\lambda\sigma_\lambda(T) \tag{S16}$$

where $\vec{e}_\lambda$ and σ are the eigenvector of phonon mode λ and the Gaussian width respectively. The σ is given by

$$\sigma_\lambda(T) = l_\lambda\sqrt{2n_\lambda(T) + 1} \quad \text{(S17)}$$

$$l_\lambda = \sqrt{\frac{\hbar}{2M_p\Omega_\lambda}} \quad \text{(S18)}$$

Where l_λ and $n_\lambda(T)$ are vibrational characteristic length and the Bose-Einstein occupation and of mode λ with frequency Ω_λ. The supercell method can be used to obtain the phonon modes. The thermal average of the Landauer conductance and the optical absorption for sufficiently large systems can be obtained using the configuration displaced as given by Eq. (S-I-8). The large system can be obtained by repeating the same smaller unit cell. Finally, the total current at temperature T and bias V can be calculated as:

$$I(V,T) = I_0[V, u_{STD}(T)] + I_{ph}[V, u_{STD}(T)] \quad \text{(S19)}$$

where I_0 is the dark current. The total current under sunlight illumination can be obtained by integrating the current over frequency with the flux *F* given by the AM1.5 reference spectrum.

References:

[i] Zhang, Ting, Rolf Heid, Klaus-Peter Bohnen, Ping Sheng, and C. T. Chan. "Phonon spectrum and electron-phonon coupling in zigzag graphene nanoribbons." *Physical Review B* 89, no. 20 (2014): 205404.

[ii] Erhart, Paul, and Karsten Albe. "Analytical potential for atomistic simulations of silicon, carbon, and silicon carbide." *Physical Review B—Condensed Matter and Materials Physics* 71, no. 3 (2005): 035211.